# Highly-efficient Polarization-insensitive Antireflection Metagrating for Terahertz Waves

Xinyu Ma[1], Yanfeng Li[1,*], Yongchang Lu[1,2], Jiaguang Han[1,*], Xixiang Zhang[2,*], and Weili Zhang[1,3]

[1]*Center for Terahertz Waves, Key Laboratory of Optoelectronic Information Technology (Ministry of Education), College of Precision Instrument and Optoelectronics Engineering, Tianjin University, Tianjin 300072, People's Republic of China*

[2]*Physical Science and Engineering Division, King Abdullah University of Science and Technology, Thuwal 23955-6900, Saudi Arabia*

[3]*School of Electrical and Computer Engineering, Oklahoma State University, Stillwater, Oklahoma 74078, USA*

*Corresponding authors: yanfengli@tju.edu.cn jiaghan@tju.edu.cn xixiang.zhang@kaust.edu.sa

**Abstract:** A simple approach based on effective medium theory is proposed and applied to evaluate and design a polarization–insensitive antireflection metagrating for terahertz waves. The period of the grating is subwavelength such that there is only one propagating mode within the grating region and high–order diffraction orders do not exist. Thus, the grating region is treated as a homogeneous medium and the whole problem can be modelled as a Fabry–Perot resonator, whose thickness then determines the transmittance. The transmittances of the fabricated device for TE and TM waves at 0.87 THz are measured to be 84% and 95% for an air–silicon surface, respectively. This simple metagrating design will find important applications in antireflection scenarios in the terahertz frequency range.

**Keywords:** Antireflection; Metamaterial; Metagrating; Effective medium theory; Terahertz wave

## 1. Introduction

Metamaterials are artificial media composed of subwavelength structures. By controlling the subwavelength units, metamaterials can control the amplitude, phase, and polarization of light, and hence can achieve many functions beyond those by traditional optical devices such as the negative refractive index [1], cloaking [2, 3], asymmetric transmission [4], planar holography [5] and so on. In cases where traditional optics works, metamaterials can often do better [6].

In recent years, terahertz (THz) waves are finding wider applications in spectroscopy [7], imaging [8], quality control [9], communications [10], and many other fields. In a typical THz system, many devices are based on high refractive index materials such as silicon and there are considerable reflection losses at an interface between air and such a material. Therefore, antireflection coatings are highly needed in the THz frequency range. In the visible region, a quarter–wave dielectric coating is typically used as an antireflection layer, whose refractive index

needs to match the square root of the product of the refractive indices of the substrate material and the incident medium. But in the THz region, corresponding dielectric materials can hardly be found [11]. Also, the long wavelength of THz waves makes antireflection coatings too thick to be easily fabricated [12, 13]. Therefore, two–dimensional (2D) pyramidal gratings are often employed for antireflection in the THz region [14-16] by forming a smooth index transition from air to the material, and they have the advantages of a wide bandwidth, high efficiency and polarization independence. However, the fabrication of 2D pyramidal gratings is difficult and especially for those structures with optimized non–smooth profiles.

In the past few years, generation and manipulation of THz waves by metamaterials have drawn considerable attention. For instance, metal–dielectric multilayer structures, split–ring resonators and many other metamaterials are used to generate THz waves [17-19]. Many functional devices including half–wave plates, beam splitters, filters and waveguide devices can be achieved with metamaterials [20-23]. In particular, 2D antireflection metamaterials have been reported [24, 25]. In contrast to 2D antireflection metamaterials, one–dimensional (1D) dielectric metagratings have the advantages of convenient design and simple fabrication. Clausnitzer *et al*. proposed dielectric grating antireflection coatings with nearly 100% diffraction efficiency [26]. However, this kind of antireflection grating is polarization–sensitive. In the meantime, simple analytical grating theories have been developed. Clausnitzer *et al.* proposed an intelligible explanation of deep–etched dielectric gratings and explained the physical processes happening in the grating [27-29] by considering the interference of only a few propagating modes inside the grating region. This simplified modal method (SMM) was further developed and applied to various device designs [30-32].

In this work, we design and fabricate a subwavelength metagrating–based polarization–insensitive antireflection structure in the THz region. Effective medium theory [33] is used to simplify the design process and verified by numerical simulation. For an air–silicon surface, the measured transmittances of the fabricated device for transverse electric (TE) and transverse magnetic (TM) waves at 0.87 THz are 84% and 95%, respectively. This grating is expected to find important applications in antireflection scenarios in the THz frequency range.

## 2. Theory analysis and design

### *2.1 Theory of simplified modal method*

Typically, 1D Gratings have different responses for TE and TM polarizations [29, 32, 33]. Here ‘polarization–insensitive antireflection’ is achieved by designing the grating parameters such that an effective Fabry–Perot resonator is formed and the transmittance reaches minimum for TE and TM waves simultaneously.

The structure of the antireflection metamaterial is a silicon–air subwavelength grating fabricated on a silicon substrate, as schematically shown in Fig.1. The grating has a period of *d*, a grating linewidth of *w*, a grating groove width of *g*, and a height of *h*. The fill factor of the grating is defined as $f = w/d$. The refractive indices of the two materials (air and silicon in this work) of the grating are $n_1$ and $n_2$, respectively.

Accurate modelling of gratings is typically done with numerical methods such as rigorous coupled wave analysis [34] and finite difference time domain method. Here we use the effective medium theory, i.e., SMM, to simplify the design process. When the period of the grating is much smaller than the incident wavelength, there can be only one propagating mode in the grating region. Other high–order modes are evanescent and can be neglected. Using effective medium theory, we can treat the subwavelength grating as a homogeneous medium and then obtain the transmittance and reflectance of the grating by applying the Fresnel's equations.

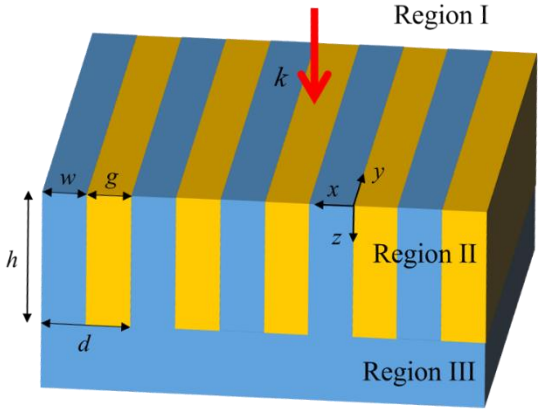


Fig. 1. Schematic of the antireflection metagrating fabricated on a high–index substrate. The grating and substrate are both made of silicon. The period of the grating is *d*=100 μm, the width of the grating ridge is *w*=50 μm, and the height of the grating is *h*=160 μm.

We will use the TM case as an example and the TE case can be treated in the same manner. A plane TM wave is assumed to be incident on the grating in the *x*-*y* plane, which means that the magnetic field is in the *y* direction. The Bloch mode for the TM wave in the grating region is [33]

$$\cos\left(k_{x,1}^{II}w\right)\cos\left(k_{x,2}^{II}g\right)-\frac{1}{2}\left(\frac{n_2^2}{n_1^2}\frac{k_{x,2}^{II}}{k_{x,1}^{II}}+\frac{n_1^2}{n_2^2}\frac{k_{x,1}^{II}}{k_{x,2}^{II}}\right)\sin\left(k_{x,1}^{II}w\right)\sin\left(k_{x,2}^{II}g\right)=\cos\left(k_0\sin\varphi_{in}d\right), \qquad (1)$$

where $k_{x,1}^{II}=k_0\sqrt{n_1^2-n_{eff,z}^2}$, $k_{x,2}^{II}=k_0\sqrt{n_2^2-n_{eff,z}^2}$ and $k_0=2\pi/\lambda$ is the wave vector in vacuum and $\varphi_{in}$ is the angle of incidence.

From (1), we can obtain $n_{eff,z}$, the effective refractive index along the *z* axis. $n_{eff,x}=n_1\sin\varphi_{in}$ is the effective refractive index along the *x* axis, arising from boundary

matching condition at the air–silicon interface. By this means, the total effective refractive index in the grating region is calculated as $n_{eff} = \sqrt{n_{eff,x}^2 + n_{eff,z}^2}$ . And the effective propagation constant in the grating region is defined as $k_{eff}^{II} = k_0 n_{eff}$ .

When we deal with a subwavelength grating whose period is much smaller the incident wavelength, there can be only one propagating mode in the grating region with all other high–order modes being evanescent. The grating layer then is modelled as a layer of homogeneous medium with an effective refractive index $n_{eff}$ as determined above and the whole problem is reduced to that of a homogeneous slab placed on the substrate.

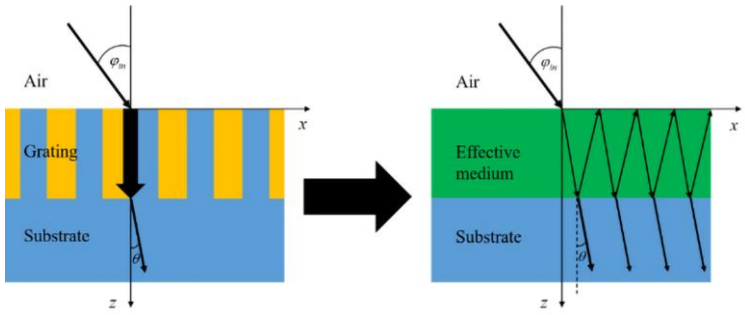


Fig. 2. Schematic illustration of SMM for modelling the grating as an effective medium with multireflection interference.

The modelling of the equivalent Fabry–Perot resonator–like structure by the SMM is illustrated in Fig. 2. The Fresnel's equations for a TM wave incident on the interface between air and the effective medium are

$$r_{TM}^{a} = \frac{n_{eff}\cos\varphi_{in} - n_1\cos\alpha}{n_{eff}\cos\varphi_{in} + n_1\cos\alpha}, \qquad t_{TM}^{a} = \frac{2n_1\cos\varphi_{in}}{n_{eff}\cos\varphi_{in} + n_1\cos\alpha} \tag{2}$$

where $\alpha$ is the angle of wave propagation in the grating.

Similarly, the reflection and transmission coefficients on the interface between the substrate and the effective medium are

$$r_{TM}^{s} = \frac{n_2\cos\alpha - n_{eff}\cos\theta}{n_2\cos\alpha + n_{eff}\cos\theta}, \qquad t_{TM}^{s} = \frac{2n_{eff}\cos\alpha}{n_2\cos\alpha + n_{eff}\cos\theta} \tag{3}$$

where $\theta$ is the angle of the wave coming out of the grating. Since there is only one propagation mode and one diffraction order in the subwavelength grating, here we use $\theta$ instead of $\theta_n$.

As the wave will experience multiple reflections as in a Fabry–Perot resonator, the effect of multireflection interference should be taken into account. Finally, we obtain the following transmission coefficient for the whole structure

$$t_{TM}^{total} = \frac{t_{TM}^{a} t_{TM}^{s}}{1 - r_{TM}^{a}{}' r_{TM}^{s} e^{i\left(\frac{4\pi}{\lambda} n_{eff} h\right)}}, \tag{4}$$

where $r_{TM}^{a}{}' = -r_{TM}^{a}$ is the reflection amplitude coefficient from the medium to air. There is π phase difference when the wave is reflected on a high–to–low refractive index interface. Also the difference in the refractive index between air, the effective homogeneous medium and the substrate must also be taken into consideration. The transmittance of the grating is finally written as

$$T = \frac{n_2 \cos\theta}{n_1 \cos\varphi_{in}} \left(t_{TM}^{total}\right)^2. \tag{5}$$

The whole grating design process based on the SMM is now basically reduced to solving the mode equation to obtain $n_{eff}$ and then use standard Fresnel formula to calculate the transmittance and reflectance. The TE case can be treated in the same way by first solving the characteristic equation for the TE wave [29,30] and then using the above Fabry–Perot analysis.

### *2.2 Validation of simplified modal method*

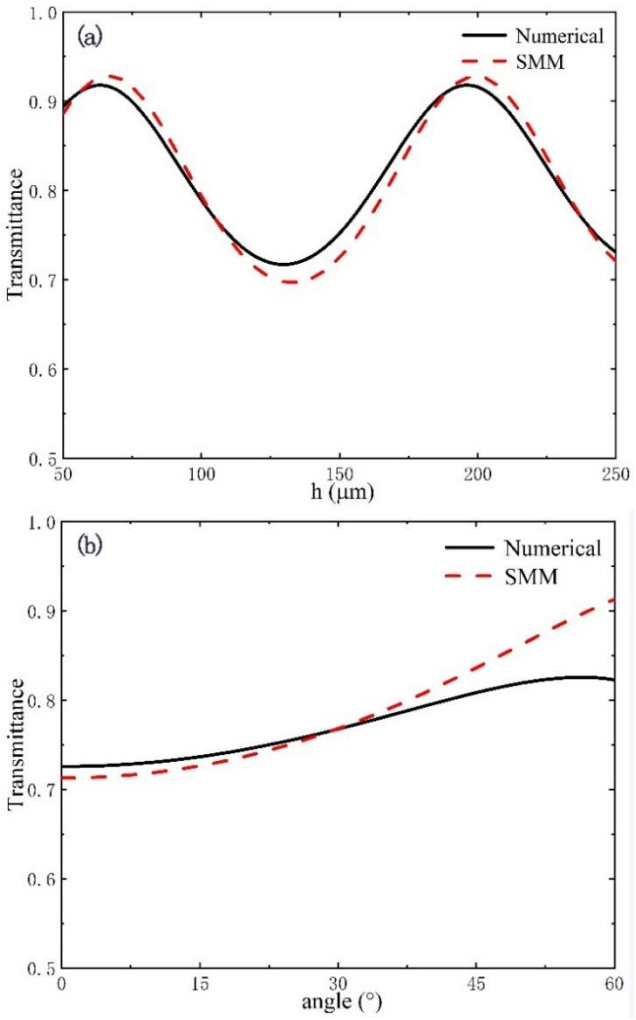


Fig. 3. (a) Transmittance versus grating groove depth. (b) Transmittance versus incident angle and $h$=120 μm is fixed. Black solid line and red dotted line represent transmittances calculated by numerical simulation and SMM, respectively.

We use a commercial simulation software COMSOL to verify the feasibility of the SMM. Here we model for the TM wave case for a silicon–air grating with parameters of $n_1$ =1, $n_2$=3.45, $d$ =50 μm and $f$ =0.5, which means that $w$=25 μm. It is assumed a plane TM wave at a frequency of 0.8 THz is vertically incident on the grating surface. Transmittances versus the depth of grating calculated by the SMM (red dotted line) and simulated by COMSOL (black solid line) are plotted in Figure 3(a), respectively. The two methods show good agreement, especially when we consider a deep subwavelength grating case here. The differences arise because evanescent modes and high–order terms of Fourier expansion are neglected in the SMM, which are found to be the main source of error in the simplified treatment [32]. Next the grating depth is fixed to be $h$=120 μm and the transmittance is investigated as a function of incident angle, as shown in Fig. 3(b). As the incident angle increases, differences between the SMM and numerical simulation become larger, but the difference is below 2% for incident angles below 45 degrees. The discrepancy at larger

incident angles is due to the fact that there is more energy distributed to high–order terms of Fourier expansion, leading to the increased error of the SMM.

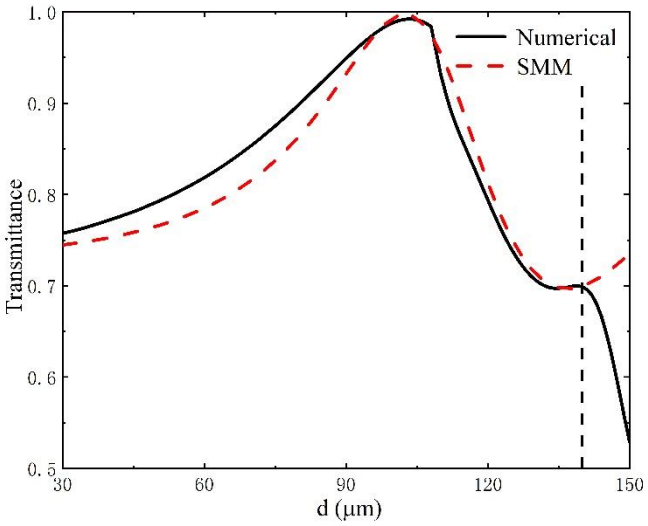


Fig. 4. Transmittance versus grating period. Black solid line and red dotted line represent transmittances simulated by numerical calculation and SMM, respectively.

Next, we investigate how the transmittance varies with the grating period. As shown in Fig. 4, the two approaches again agree well with each other until *d* is larger than 140 μm. The numerical results indicate that the SMM overestimates the grating efficiency because there are now two propagating modes in the grating region and they both need to be taken into account.

Overall, our comparisons show that the SMM can predict the grating efficiency very accurately when there is only one propagating mode in the grating region and one diffraction order outside the grating.

### *2.3 Antireflection grating design*

Having established the validity of the SMM, we now use it to design polarization–insensitive 1D antireflection gratings. The 1D gratings will be much simpler to fabricate than 2D pyramidal gratings. As is well known, 1D gratings, however, have different responses for TE and TM waves. When it comes to reverse design, the SMM will greatly facilitate the design process. Under a

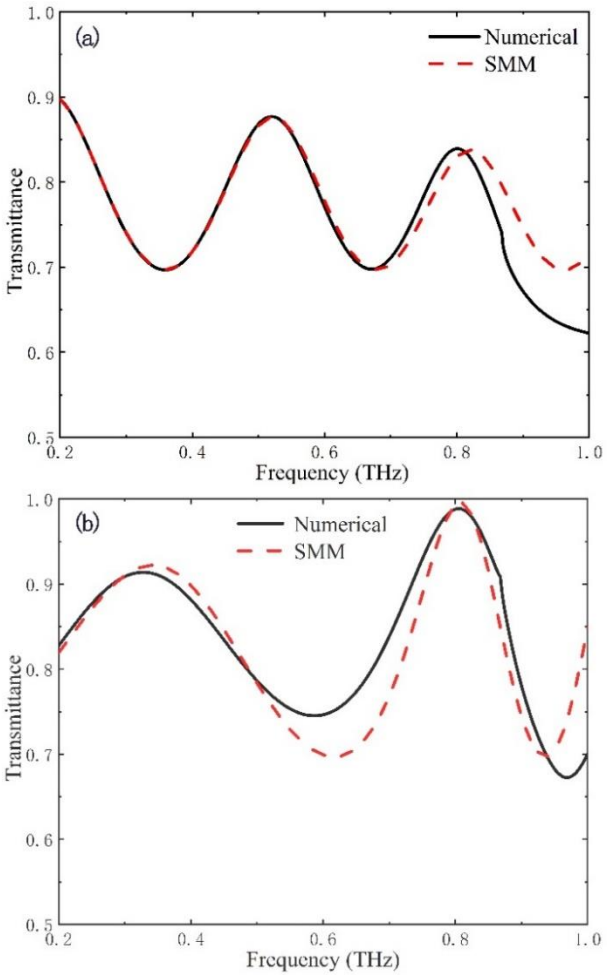


Fig. 5. Transmittance versus frequency for (a) TE and (b) TM polarization. Grating parameters are fixed as $d$=100 μm, $f$=0.5, and $h$=160 μm. Black solid line and red dotted line represent transmittance calculated by numerical simulation and SMM, respectively.

selected grating period to avoid high–order diffraction, we calculate the different effective refractive indices for TE and TM waves at 0.8 THz through a series of gratings with different fill factors. Then the groove depths for maximum transmittance of the gratings corresponding to different fill factors and polarizations can be easily obtained by the SMM. What we need to do is choose a set of fill factors and the corresponding groove depths that are close and work for both TE and TM polarizations. Then COMSOL is used to sweep the parameters nearby in order to get more precise parameters. For convenience of fabrication, the grating period is chosen as $d$=100 μm. Following the procedure described above, we find that when the fill factor is $f$ =0.5 and the groove depth is $h$=160 μm, the transmittances of the grating for both TE and TM polarizations achieve maximum, which are 85% and 99%, respectively. The results calculated by the SMM and COMSOL are compared in Fig. 5. It can be seen that the two methods agree well and transmittance maxima are obtained at 0.8 THz for both TE and TM waves. For a homogeneous antireflection layer, only when the effective refractive index satisfies $n_{eff} = \sqrt{n_1 n_2}$ can all the

incident wave propagate through it. However, $n_{eff}^{TM}$ and $n_{eff}^{TE}$ cannot meet the condition simultaneously. Here only $n_{eff}^{TM}$ is chosen to meet the condition. So the transmittance of the TM wave achieves 99% in theory and that of the TE wave achieves 85%.

## 3. Experimental Results

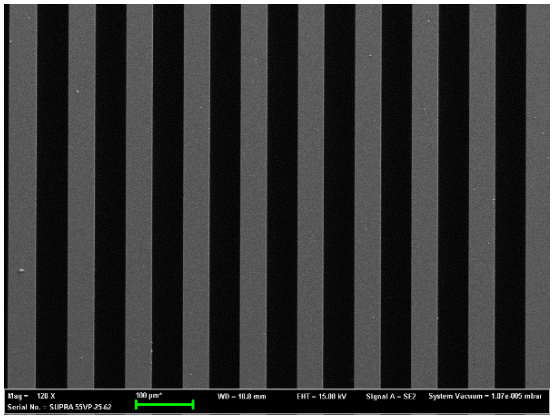

Fig. 6. Scanning electron microscopy image of antireflection grating.

The grating designed as above is fabricated and experimentally tested. Figure 6 shows the scanning electron microscopy image of the fabricated silicon–air grating. The silicon–air grating was manufactured by lithography and deep reactive ion etching. First, the designed pattern was imported into a laser writer to fabricate the mask. The second step was to pre–process the silicon wafer by heating and washing. Next, a 10 μm–thick positive photoresist film (AZ9260) was spin–coated on the wafer. After lithography, the wafer was developed in AZ726 developer for six minutes and then washed by deionized water. Next deep reactive ion etching with $SF_6$ (for etching silicon) and $C_4F_8$ (for protecting the sidewall) was used to etch the wafer to form the grating. Finally, the remaining photoresist was removed by acetone. A THz time–domain spectroscopy system was used to measure the far–field transmittance of the grating.

The theoretical and experimental transmission efficiencies of the grating are compared in Fig. 7. In general, the objective for a high–efficiency polarization–insensitive antireflection grating design is achieved. The transmittance of the grating for the TE wave achieves 84% and that for the TM wave achieves 94% at 0.87 THz in the experiment. The results show that through the designed metagrating the reflectance at a single silicon–air interface is reduced from 30% to 15% for the TE wave and 5% for the TM wave.The discrepancy between the design and the experiment comes mainly from the fabrication error in the grating parameters. Our designed grating period is $d$=100 μm, fill factor $f$ =0.5, groove depth is $h$=160 μm, and the refractive index of silicon is assumed to

be $n_2$=3.45. But the actual grating period is $d$=101 μm, fill factor is $f$ =0.47, groove depth is $h$=144 μm, and the refractive index of silicon is measured to be $n_2$=3.38. The lower grating depth causes

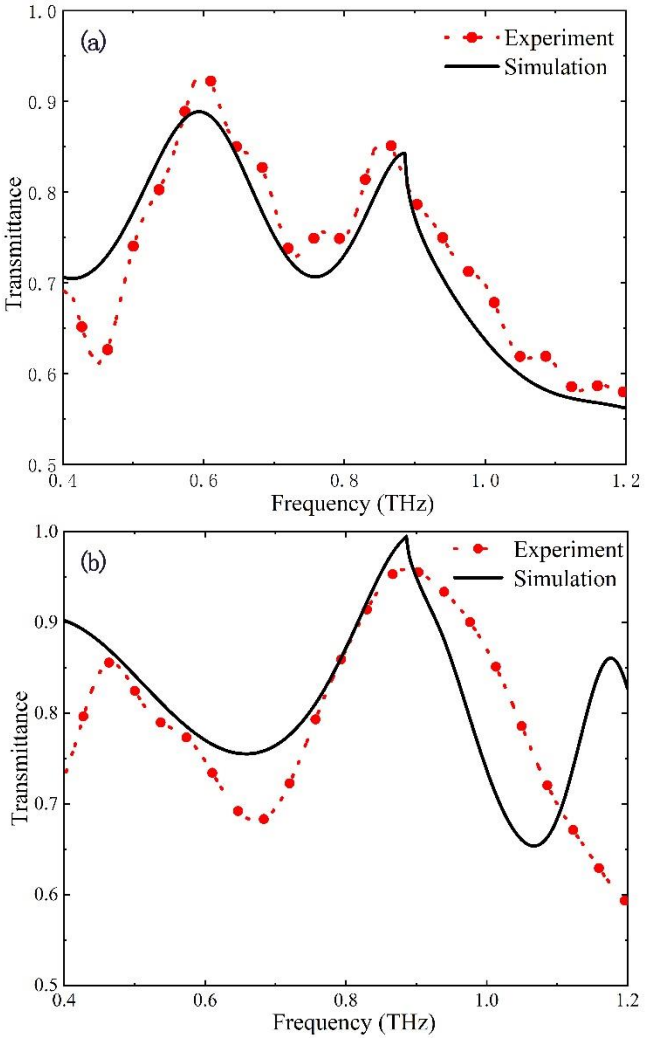


Fig. 7. Theoretical and experimental diffraction efficiencies of metagrating versus frequency for (a) TE and (b) TM wave. Black solid line and red dotted line represent simulation and experimental results, respectively.

a blue shift of the maximum transmittance to occur at 0.87 THz. The bandwidth is also narrower than design, and this is due to the fact that higher–order diffraction orders begin to appear for above 0.9 THz such that the transmittance decreases rapidly.

## 4. Conclusion

We have designed and fabricated a polarization–insensitive antireflection metagrating with a transmittance of 84% for TE polarization and transmittance of 94% for TM polarization at 0.87 THz. The reflectance at a single silicon–air interface is reduced from 30% to 15% for TE wave and 5% for TM wave. The metagrating is designed by analytical effective theory and verified by numerical calculation, and it greatly simplifies the inverse design procedure. The reported 1D

groove grating has the advantages of simple design and easy fabrication and will be of use in THz systems where antireflection is desirable. The methodology may also find applications in other similar 1D grating designs.

## Acknowledgments

The authors are grateful to Fan Yang of Tsinghua University for valuable discussions. This work was supported by the National Key Research and Development Program of China (Grant No. 2017YFA0701004), the Tianjin Municipal Fund for Distinguished Young Scholars (Grant No. 18JCJQJC45600), the National Natural Science Foundation of China (Grant Nos. 61775159, 61420106006, 61427814, 61422509, 61735012, and 61505146), and King Abdullah University of Science and Technology (KAUST) Office of Sponsored Research (OSR) (Grant No. OSR-2016-CRG5-2950).

## References

[1] Smith D R, Padilla W J, Vier D C, Nemat-Nasser S C and Schultz S, Composite Medium with Simultaneously Negative Permeability and Permittivity, *Phys. Rev. Lett.* 84 (2000) 4184-87. https://doi.org/10.1103/PhysRevLett.84.4184.

[2] Schurig D, Mock J J, Justice B J, Cummer S A, Pendry J B, Starr A F and Smith D R, Metamaterial Electromagnetic Cloak at Microwave Frequencies, *Science*. 314 (2006) 977-980. https://doi.org/10.1126/science.1133628.

[3] Huang Y, Feng Y, Jiang T, Electromagnetic cloaking by layered structure of homogeneous isotropic materials, *Opt. Express*. 15 (2007) 11133-11141. https://doi.org/10.1364/OE.15.011133.

[4] Fedotov V A, Mladyonov P L, Prosvirnin S L, Rogacheva A V, Chen Y and Zheludev N I, Asymmetric propagation of electromagnetic waves through a planar chiral structure, *Phys. Rev. Lett.* 97 (2006) 167401. https://doi.org/10.1103/PhysRevLett.97.167401.

[5] Li A, Singh S, Sievenpiper D, Metasurfaces and their applications, *Nanophotonics* 7 (2018) 989-1011. https://doi.org/10.1515/nanoph-2017-0120.

[6] Smith D R, Schurig D, Mock J J, Kolinko P and Rye P, Partial focusing of radiation by a slab of indefinite media, *Appl. Phys. Lett.* 84 (2004) 2244-2246. https://doi.org/10.1063/1.1690471.

[7] Yang X, Zhao X, Yang K, Liu Y, Fu W and Luo Y, Biomedical applications of terahertz spectroscopy and imaging, *Trends Biotechnol.* 34 (2016) 810-824. https://doi.org/10.1016/j.tibtech.2016.04.008.

[8] Federici J F, Schulkin B, Huang F, Gary D, Barat R, Oliveira F and Zimdars D, THz imaging and sensing for security applications—explosives, weapons and drugs, *Semicond. Sci. Technol.* 20 (2005) 266-280. https://doi.org/10.1088/0268-1242/20/7/018/meta.

[9] Gowen A A, C. O'Sullivan, C.P. O'Donnell, Terahertz time domain spectroscopy and imaging: Emerging techniques for food process monitoring and quality control, *Trends Food Sci. Technol.* 25 (2012) 40-46. https://doi.org/10.1016/j.tifs.2011.12.006.

[10] Federici J, Moeller L, Review of terahertz and subterahertz wireless communications, *J. Appl. Phys.* 107 (2010) 111101. https://doi.org/10.1063/1.3386413.

[11] Lai W, Born N, Schneider L M, Rahimi-lman A, Balzer J C and Koch M, Broadband antireflection coating for optimized terahertz beam splitters, *Opt. Mater. Express* 5 (2015) 2812-2819. https://doi.org/10.1364/OME.5.002812.

[12] Gatesman A J, Waldman J, Ji M, Musante C and Yagvesson S, An anti-reflection coating for silicon optics at terahertz frequencies, *IEEE Microwave Guided Wave Lett.* 10 (2000) 264-266. https://doi.org/10.1109/75.856983

[13] Hosako I, Multilayer optical thin films for use at terahertz frequencies: method of fabrication, *Appl. Opt.* 44 (2005) 3769-3773. https://doi.org/10.1364/AO.44.003769.

[14] Han P, Chen Y W, Zhang X C, Application of silicon micropyramid structures for antireflection of terahertz waves, *IEEE J. Sel. Top. Quantum Electron.* 16 (2009) 338-343. https://doi.org/10.1109/JSTQE.2009.2031164.

[15] Li X, Hu X, Li Y and Chai L, A three-step procedure for the design of broadband terahertz antireflection structures based on a subwavelength pyramidal-frustum grating, *J. Lightwave Technol.* 32 (2014) 1463-1471. https://doi.org/10.1109/JLT.2013.2296295.

[16] Hu X, Li Y, Fang F, Li X, Li J, Chen Y, Zhang X, Chai L, Wang C, Fedotov A B and Zheltikov A M, Enhancement of terahertz radiation from GaP emitters by subwavelength antireflective micropyramid structures, *Opt. Letters* 38 (2013) 2053-2055. https://doi.org/10.1364/OL.38.002053.

[17] Musin R, Xing Q, Li Y, Hu M, Chai L, Wang Q, Mikhailova Y M, Nazarov M M, Shkurinov A P and Zheltikov A M, Design rules for phase-matched terahertz surface electromagnetic wave generation by optical rectification in a nonlinear planar waveguide, *Appl. Opt.* 47 (2008) 489-494. https://doi.org/10.1364/AO.47.000489.

[18] Luo L, Chatzakis I, Wang J, Niesler F B, Wegener M, Koschny T, and Soukoulis C M, Broadband terahertz generation from metamaterials, *Nat. Commun.* 5 (2014) 3055. https://doi.org/10.1038/ncomms4055.

[19] Minerbi E, Keren-Zur S, and Ellenbogen T, Nonlinear metasurface Fresnel zone plates for terahertz generation and manipulation, *Nano Lett.* 19 (2019) 6072-6077. https://doi.org/10.1021/acs.nanolett.9b01970.

[20] Zi J, Xu Q, Wang Q, Tian C, Li Y, Zhang X, Han J and Zhang W, Antireflection-assisted all-dielectric terahertz metamaterial polarization converter. *Appl. Phys. Lett*. 113 (2018) 101104. https://doi.org/10.1063/1.5042784.

[21] Xing X, Li Y, Lu Y, Zhang W, Zhang X, Han J and Zhang W, Terahertz metamaterial beam splitters based on untraditional coding scheme, *Opt. Express* 27 (2019), A1627-A1635. https://doi.org/10.1364/OE.27.0A1627.

[22] Niu Q, Tang C, He Y, Hu L and Wang B X, Design of multiple-band filtering resonance devices at narrow frequency range using terahertz metamaterial resonator, *Opt. Commun.* 453 (2019) 124368. https://doi.org/10.1016/j.optcom.2019.124368.

[23] Yuan M, Li Y, Lu Y, Zhang Y, Zhang Z, Zhang X, Zhang X, Han J and Zhang W, High-performance and compact broadband terahertz plasmonic waveguide intersection. *Nanophotonics*, 8 (2019), 1811-1819. https://doi.org/10.1515/nanoph-2019-0191.

[24] Brückner C, Käsebier T, Pradarutti B, Riehemann S, Notni G, Kley E B and Tünnermann A, Broadband antireflective structures applied to high resistive float zone silicon in the THz spectral range, *Opt. Express* 17 (2009) 3063-3077. https://doi.org/10.1364/OE.17.003063.

[25] Chen H T, Zhou J, O'Hara J F, Chen F, Azad A K and Taylor A J, Antireflection coating using metamaterials and identification of its mechanism, *Phys. Rev. Lett.* 105 (2010) 073901. https://doi.org/10.1103/PhysRevLett.105.073901.

[26] Clausnitzer T, Kaempfe T, Kley E B, Tünnermann A, Tishchenko A V and Parriaux O, Highly-dispersive dielectric transmission gratings with 100% diffraction efficiency, *Opt. Express* 16 (2008) 5577-5584. https://doi.org/10.1364/OE.16.005577.

[27] Clausnitzer T, Kämpfe, T, Kley E B, Tünnermann A, Peschel U, Tishchenko A V and Parriaux O, An intelligible explanation of highly-efficient diffraction in deep dielectric rectangular transmission gratings, *Opt. Express* 13 (2005) 10448-10456. https://doi.org/10.1364/OPEX.13.010448.

[28] Foresti M, Menez L, Tishchenko A V, Modal method in deed metal-dielectric gratings: the decisive role of hidden modes, *J. Opt. Soc. Am. A* 23 (2006) 2501-2509. https://doi.org/10.1364/JOSAA.23.002501.

[29] Clausnitzer T, Kämpfe, Thomas, Kley E B, Tünnermann A, Tishchenko A V and Parriaux O, Investigation of the polarization-dependent diffraction of deep dielectric rectangular transmission gratings illuminated in Littrow mounting, *Appl. Opt.* 46 (2007) 819-826. https://doi.org/10.1364/AO.46.000819.

[30] Sun W, Lv P, Zhou C, Cao H and Wu J, Multireflection modal method for wideband fused-silica transmission gratings, *Appl. Opt.* 52 (2013) 2800-2807. https://doi.org/10.1364/AO.52.002800.

[31] Zheng J, Zhou C, Wang B and Feng J, Beam splitting of low-contrast binary gratings under second Bragg angle incidence, *J. Opt. Soc. Am. A* 25 (2008) 1075-1083. https://doi.org/10.1364/JOSAA.25.001075.

[32] Yang F, Li Y, Evaluation and improvement of simplified modal method for designing dielectric gratings, *Opt. Express* 23 (2015) 31342-31356. https://doi.org/10.1364/OE.23.031342.

[33] Tang S, Zhu B, Jia M, He Q, Sun S, Mei Y and Zhou L, Effective-medium theory for one-dimensional gratings, *Phys. Rev. B* 91 (2015) 174201. https://doi.org/10.1103/PhysRevB.91.174201.

[34] Moharam M G and Gaylord T K, Rigorous coupled-wave analysis of planar-grating diffraction, *J. Opt. Soc. Am.* 71 (1981) 811-818. https://doi.org/10.1364/JOSA.71.000811.